

Article

Pseudomonas syringae Infection Modifies Chlorophyll Fluorescence in *Nicotiana tabacum*

Magdalena Tomaszewska-Sowa ^{1,*}, Norbert Keutgen ^{1,2} , Tomáš Lošák ³, Anna Figas ¹  and Anna J. Keutgen ² 

¹ Department of Agricultural Biotechnology, Bydgoszcz University of Science and Technology, Bernardyńska 6, 85-029 Bydgoszcz, Poland

² Department of Crop Sciences, Institute of Vegetables and Ornamentals, University of Natural Resources and Life Sciences, Gregor Mendel Str. 33, 1180 Vienna, Austria

³ Department of Environmentalistics and Natural Resources, Faculty of Regional Development and International Studies, Mendel University in Brno, Zemědělská 1, 613 00 Brno, Czech Republic

* Correspondence: magda@pbs.edu.pl

Abstract: The system *Nicotiana tabacum* L.—*Pseudomonas syringae* VAN HALL pv. *tomato* (Pto) DC3000 was investigated at a low inoculation level (c. 5×10^5 colony-forming units (CFU) mL⁻¹) such as it occurs in the field. The aim of this study was to test the hypothesis that *N. tabacum*, a non-host of Pto DC3000, improved the PSII efficiency in inoculated leaves compared with control detached leaves. Visible symptoms at the infected area were not detected within 14 days. Chlorophyll (Chl) *a* fluorescence was measured 6–7 days after inoculation of detached leaves. Compared with the control, the actual photochemical quantum yield of photosystem (PS) II was higher in the inoculated leaves at the expense of the fraction of heat dissipated by photo-inactivated non-functional centers. In addition, the fraction of open PSII reaction centers (RCs) was higher in inoculated leaves. Maximum fluorescence in the dark-adapted detached inoculated leaves, as a measure of the absorbed energy, was lower than in control leaves. The lower capacity to absorb energy in combination with a higher fraction of open PSII RCs is interpreted as an acclimation to limit over-excitation and to reduce heat dissipation. This should limit the production of reactive oxygen species and reduce the probability of a hypersensitive response (HR), which represents an expensive cell-death program for the plant.

Keywords: *Pseudomonas syringae* VAN HALL pv. *tomato* DC3000; *Nicotiana tabacum* L.; steady state fluorometry; incompatible host plant—pathogen interaction; leaf detachment



Citation: Tomaszewska-Sowa, M.; Keutgen, N.; Lošák, T.; Figas, A.; Keutgen, A.J. *Pseudomonas syringae* Infection Modifies Chlorophyll Fluorescence in *Nicotiana tabacum*. *Agriculture* **2022**, *12*, 1504. <https://doi.org/10.3390/agriculture12091504>

Academic Editors: Beatrice Berger and Matthias Becker

Received: 19 July 2022

Accepted: 13 September 2022

Published: 19 September 2022

Publisher's Note: MDPI stays neutral with regard to jurisdictional claims in published maps and institutional affiliations.



Copyright: © 2022 by the authors. Licensee MDPI, Basel, Switzerland. This article is an open access article distributed under the terms and conditions of the Creative Commons Attribution (CC BY) license (<https://creativecommons.org/licenses/by/4.0/>).

1. Introduction

Strains of *P. syringae* are noted for their diverse and host-specific interactions with plants and may be assigned to one of at least 50 pathovars based on host specificity. Host plants of the corresponding pathovar develop lesions and chlorotic halos, while non-host and resistant plants develop an HR, characterized by a rapid cell death. Non-host resistance refers to the resistance of a plant species to a pathogen and contrasts with host resistance (race-specific resistance), which is achieved by a special genotype within a host species. Typically, it protects only from a selected genotype of the pathogen [1]. Within the non-host resistance, two types can be distinguished: type I, where the HR is not elicited, and type II, where the HR is triggered. In the case of *P. syringae* pathovars, the latter type of non-host resistance dominates [2]. As a matter of fact, type-II non-host and host resistance against *P. syringae* often show a similar appearance. When inoculated with high levels of *P. syringae*, a rapid tissue collapse typical of the HR is observed in both. *N. tabacum* is a non-host of *P. syringae* pv. *tomato* (Pto) DC3000 [1], similar to *N. benthamiana* DOMIN, which does not show any HR symptoms when inoculated at a low level, but responds with the HR at a high level [2].

Several studies focused on the light reactions of photosynthesis in plant-pathogen interactions. In summary, irrespective of infection type, the most common responses

were a decrease in ϕ_{P0} and ϕ_P [3–5], while that of non-photochemical quenching was variable, depending on the time of measurement after infection and the position of the measurement [4,5]. While plant responses to high inoculation levels of *Pseudomonas* are well known, less information is available on lower levels, although this may be the more frequent case of infection in nature. In the case of a compatible interaction (host plant—pathogen interaction, the ϕ_P and NPQ in *Phaseolus vulgaris* L.—*Pseudomonas syringae* pv. *phaseolicola* 1448A) were significantly reduced in the non-infected area 5 days after inoculation, whereas inoculation of *P. vulgaris* with Pto DC3000 (incompatible interaction) did not result in any detectable effect for Chl fluorescence [6]. The present study also aimed at investigating the effect of a low inoculation level in *N. tabacum* leaves with Pto DC3000 (incompatible interaction), in order to elucidate the response of the photosynthetic system when visible damage and Chl degradation do not occur. It is hypothesized that such an approach should detect responses that are otherwise concealed by processes associated with the rapid death of cells in the infected leaf area.

Various aspects were reported to play a significant role in the susceptibility of a host plant to a pathogen. Among these are special calcium sensors [7], signaling by reactive oxygen species [8], hormonal interactions [9] and molecule priming [10], which all together modify gene transcription and physiological responses in the host plant [11,12]. For crop production, knowledge of these responses is of prime importance in order to control the distribution of diseases. However, novel and eco-friendly approaches are requested by the public in disease management [11,13]. A successful strategy was the selection of abiotic stress-tolerant varieties and integrated pest management applying pesticides respecting public health and also the environment under the climate-change scenario [11]. In addition, it was found that indigenous microbial communities are involved in maintaining plant health [14]. Hence, the application of living organisms may constitute a potentially important approach in sustainable agriculture to control disease. For instance, Hanemian et al. [15] suggested controlling the main gram-negative phytopathogenic bacteria-induced diseases by inoculating host plants with bacteria strains mutated in *hrp* (hypersensitive response and pathogenicity) genes. The application of these mutants indeed reduced, or completely abolished, disease symptoms in several host plant—pathogen systems involving the main gram-negative phytopathogenic bacteria *P. syringae*, *Ralstonia solanacearum* (SMITH), *Erwinia amylovora* (BURRILL), and *Xanthomonas campestris* DOWSON [15]. However, the concerns of the public against genetic manipulation in agriculture may limit this approach [16]. Consequently, it is here suggested that studies focus on incompatible crop plant—pathogen interactions, because such interactions represent a potential goal for any kind of crop plant—pathogen interaction, considering the concept of sustainable agriculture.

2. Materials and Methods

2.1. Plant Material and Inoculation of Tobacco Leaves

Tobacco (*N. tabacum* cv. Bursan) seeds were cultivated in plastic pots with potting soil at a light intensity of c. 90 $\mu\text{mol photons m}^{-2} \text{s}^{-1}$ (Philips-TLD36 W/840, Amsterdam, The Netherlands) with a 16:8 h day/light regime, temperature of $24/20 \pm 2$ °C, and air humidity of c. 85–90% in a phytotron. For the inoculation experiment, completely expanded leaves at growth stage 1108 [17] were detached and the youngest completely developed leaf was used. It was either treated with Pto DC3000 or with demineralized water as a control. For comparison, measurements were also performed on non-inoculated attached leaves at the same growth stage on plants cultivated under the same environmental conditions in order to evaluate the effect of leaf detachment on Chl-fluorescence parameters.

It was decided to inoculate detached leaves for the present study, because preliminary tests applying higher concentrations of inoculum (c. 1×10^7 CFU mL^{-1}) onto attached leaves resulted in a quite variable inoculation success, whereas inoculation of detached leaves revealed comparable results rated by the appearance of chlorotic and necrotic spots. Because inoculation with a low level of inoculum did not result in visible symptoms, it was decided to perform the experiment on detached leaves, taking advantage of the

more consistent inoculation success. Preliminary Chl-fluorescence measurements indicated treatment effects and justified the selected lower inoculation concentration for studying the incompatible crop plant—pathogen interaction at a level that is considered more typical for an infection under natural environmental conditions.

Table 1. Definition of fluorescence parameters of the saturation pulse and steady-state fluorometry after Oxborough and Baker [18], Murchie and Lawson [19] and Lazar [20].

Chl-Fluorescence Parameters	Meaning
F_0	Minimum fluorescence when all RCs are open at the onset of fluorescence induction
F_m	Maximum fluorescence when all RCs are closed
$F_v = F_m - F_0$	Maximum variable fluorescence
$\varphi_{P0} = F_v / F_m$	Maximum quantum efficiency of PSII
$F_0' = F_0 / [(F_v / F_m) + (F_0 / F_m)']$	Minimum fluorescence for the light-adapted state
F_m'	Maximum fluorescence for the light-adapted state
F'	Actual (stationary) fluorescence during the slow fluorescence induction
$F_v' = F_m' - F_0'$	Variable fluorescence for a light-adapted state
$\Delta F = F_m' - F'$	Difference in fluorescence between F_m' and F'
$\varphi_{PSII} = F_v' / F_m'$	Maximum efficiency of PSII photochemistry for the light-adapted state, if all centers are open
$q_P = \Delta F / F_v'$	Photochemical quenching coefficient
$q_L = q_P / (F_0' / F')$	Estimate of the fraction of open PSII RCs
$NPQ = (F_m - F_m') / F_m'$	Non-photochemical Chl fluorescence quenching
$PQ = F_m / F' - F_m / F_m'$	Photochemical Chl fluorescence quenching
Energy Partitioning	Meaning
$\varphi_P = \Delta F / F_m' = \varphi_{PSII} \times q_P$	Actual photochemical quantum yield of PSII photochemistry for the light-adapted state
$\varphi_{NPQ1} = F' / F_m' - F' / F_m$	Quantum yield of regulatory non-photochemical quenching after Genty et al., Cailly et al. and Hendrickson et al. [21–23]
$\varphi_{NPQ2} = (1 - (\varphi_{PSII} / 0.8)) \times (F' / F_0')$	Quantum yield of regulatory non-photochemical quenching after Kornyejev and Holaday [24]
$\varphi_{\text{t,D}1} = F' / F_m$	Quantum yield of constitutive non-regulatory basal dissipation processes consisting of fluorescence emission and heat dissipation after Genty et al., Cailly et al. and Hendrickson et al. [21–23]
$\varphi_{\text{t,D}2} = (F' / F_m') + (\varphi_{PSII} / \varphi_{P0}) \times (F' / F_0') - (F' / F_0')$	Quantum yield of constitutive non-regulatory basal dissipation processes consisting of fluorescence emission after Kornyejev and Holaday [24]
$\varphi_{NF2} = (1 - (0.8 / \varphi_{P0})) \times (\varphi_{PSII} / 0.8) \times (F' / F_0')$	Quantum yield of heat dissipation by the photo-inactivated non-functional centers after Kornyejev and Holaday [24]

Pto DC3000 was cultivated on King's B agar plates at 28 °C. The bacteria were suspended in sterile, demineralized water. An optical density of c. 0.2, measured spectrophotometrically at 630 nm, corresponded to c. 1×10^8 CFU mL⁻¹. The suspension was diluted to a concentration of c. 5×10^5 CFU mL⁻¹ for the application. A 1-mL needleless syringe was used to pressure-infiltrate the abaxial side of the leaf; control leaves were treated similarly with demineralized water. As suggested by Kalaji et al. [25], the detached inoculated leaves were laid on wet tissue paper and the petiole plus the lower third of the leaves were covered with another sheet of wet tissue paper. The leaves were kept in darkness at c. 20 °C and c. 95% relative humidity for c. 16 h, and were then transferred, together with the wet tissue paper, to the phytotron and exposed to the mentioned environmental conditions. The tissue was kept wet with demineralized water three times a day. The inoculated and control leaves were kept in the phytotron for the following 6–7 days until measurement. This period of time was selected because Rodríguez-Moreno et al. [6] observed an effect when applying Chl fluorescence in the case of the compatible interaction *Phaseolus vulgaris*—*P. syringae* pv. *phaseolicola* 1448A, not earlier than 5–7 days after inoculation, with a low level of inoculum. After the measurements, the inoculated leaves remained in the phytotron for 14 days in order to demonstrate whether chlorotic or necrotic spots appeared during the second week after inoculation. Some 75 leaves per variant were inoculated for the experiment.

2.2. Chl *a* Fluorescence Procedures

Chl-fluorescence measurements were performed with the PAM-2500 (Heinz Walz GmbH, Effeltrich, Germany) in three independent experimental replicates, 6–7 days after detachment and infiltration. Measurements were taken on the same half of the leaf (divided by the midrib into two equal halves) where the inoculation took place, but in the non-infiltrated area, c. 1 cm apart towards the leaf tip. For the saturation pulse, steady-state fluorescence and ‘JIP’ measurements, leaves were dark-adapted in an accordingly designed box. Recommended times for dark adaptation vary from 15 to up to 30 min [25–27]. For the current experiment, a dark adaptation of 20 min was selected, which ensured the relaxation of the transthylakoid pH difference, inactivation of the ferredoxin NADP reductase, and realignment of the chloroplasts within the cell [26]. In the case of the combined saturation pulse and steady-state fluorescence, measurements started with a modulated measuring beam to determine minimum fluorescence (F_0). A saturating pulse of red light ($10,000 \mu\text{mol m}^{-2} \text{s}^{-1}$) was then applied to measure maximum fluorescence (F_m). Actinic red light (red LEDs with a maximum emission at 630 nm, FWHM 15 nm, PAR of $925 \mu\text{mol photon m}^{-2} \text{s}^{-1}$) was switched on and saturation pulses were applied every 20 s for 5 min to measure the adaptation of the light reactions of photosynthesis to the applied actinic light intensity following changes of maximum fluorescence in the light-adapted state (F_m'), and actual fluorescence during the slow fluorescence induction (F') under the actinic light. The shapes of the response curves indicated that the measurements at the end of the 5 min period could be used for further calculations, because an almost steady state was reached.

The measurement of the Kautsky induction curves (‘JIP’ analysis) was, in principle, identical to the measurement of the F_0 and F_m of the saturation pulse measurement, but data were recorded every 10 μs . The measurement started with a modulated measuring beam with a photon irradiance of $0.1 \mu\text{mol (photon) m}^{-2} \text{s}^{-1}$ to assess F_0 . The measuring light was supplied by red LEDs, with a maximum emission at 630 nm and FWHM (full width half max) of 20 nm (1 μs pulses at 200 Hz modulation frequencies for the determination of F_0). A saturating pulse of red light (red LEDs, maximum emission at 630 nm, FWHM 15 nm, PAR of $10,000 \mu\text{mol (photon) m}^{-2} \text{s}^{-1}$) followed, and measurements were taken every 10 μs . The measured curves were smoothed using the method of the simple moving average, as described in Keutgen et al. [28]. For the visualization of the ‘JIP’ fluorescence rise, a logarithmic time scale was used, as suggested by Kalaji et al. [25]. F_0 was recorded at the onset of fluorescence induction ($t = 0$). The ‘J’ step was taken at 2.0 ms and the ‘I’ step at 30 ms after illumination, while the ‘P’ step (F_m) was the maximum value recorded at 150, 200, or 250 ms. The derived Chl-fluorescence indices were calculated in line with Strasser et al. [29,30] and Stirbet et al. [31]. Since differences exist among authors for the calculation of M_0 , the initial slope of the F_0 –J fluorescence rise (in ms^{-1}), it is necessary to mention that it was calculated as:

$$M_0 = (\Delta V / \Delta t)_0 \cong 4(F_{0.3\text{ms}} - F_0) / F_V. \quad (1)$$

For the combined saturation pulse and steady-state fluorescence measurements, 24 replicates each were realized for the control and infected detached leaves, and also for the attached control leaves; whereas for the ‘JIP’ analyses, 40 measurements for the infected and control detached leaves were taken. The experiment was repeated independently three times. Each replication of the time-consuming steady-state fluorescence measurements consisted of 8 measurements for each of the three variants, viz. 24 measurements (=8 sets of measurements) per replication. One set of measurements consisted of (a) a detached control leaf, (b) a detached inoculated leaf and (c) an attached control leaf, the order within each set being determined by chance. Each measurement lasted for c. 30 min (20 min dark adaptation plus 5 min per measurement), which totals 12 h. The measurements were performed on two successive days, with 6 sets being measured the first and 2 sets the second day (9 h plus 3 h). Consequently, it was necessary to prepare this

experiment independently three times in order to produce a sufficient number of replicates. The derived Chl-fluorescence parameters of the saturation pulse and steady-state fluorometry are summarized in Table 1 and the additional parameters of the ‘JIP’ Chl transient analysis are found in Table 2.

Table 2. Definition of energy fluxes and fluorescence parameters of the ‘JIP’ Chl-transient fluorometry after Strasser et al. and Stirbet et al. [29,31] as far as not mentioned in Table 1.

Chl-Fluorescence Parameters	Meaning
$V_t = (F_t - F_0)/F_v$	Relative variable fluorescence, e.g., at the ‘J’ (t = 2 ms) and ‘I’ steps (t = 30 ms)
$M_0 = (\Delta V/\Delta t)_0 \cong 4(F_{0.3ms} - F_0)/F_v$	Initial slope (in ms^{-1}) of the F_0 -J fluorescence rise
Efficiencies and Quantum Yields	Meaning
$\psi_{E0} = 1 - V_J$	Efficiency with which a PSII-trapped electron is transferred from quinone $A^- (Q_A^-)$ to plastoquinone
$\varphi_{E0} = \varphi_{P0} \times \psi_{E0}$	Quantum yield of electron transport from Q_A^- to plastoquinone
$\psi_{R0} = 1 - V_I$	Efficiency with which a PSII-trapped electron is transferred to final PSI acceptors
$\varphi_{R0} = \varphi_{P0} \times \psi_{R0}$	Quantum yield of electron transport from Q_A^- to final PSI acceptors
$\delta_{R0} = \psi_{R0}/\psi_{E0}$	Efficiency with which an electron from plastoquinol is transferred to final PSI acceptors
Specific Energy Fluxes (per Active PSII)	Meaning
$ABS/RC = (M_0/V_J)/\varphi_{P0}$	Absorption flux of antenna Chls per RC; apparent antenna size of an active PSII
Performance Indexes	Meaning
$PI_{ABS} = (RC/ABS) \times [\varphi_{P0}/(1 - \varphi_{P0})] \times [\psi_{E0}/(1 - \psi_{E0})]$	Performance index for energy conservation of photons absorbed by PSII to the reduction in intersystem electron acceptors
$PI_{Total} = PI_{ABS} \times [\delta_{R0}/(1 - \delta_{R0})]$	Performance index for energy conservation from photons absorbed by PSII to the reduction in PSI end acceptors
Transformation of RCs to So-Called Silent RCs	Meaning
$RC_{si}/RC_{at} = 100 \times (1 - (ABS/RC_{at})/(ABS/RC_{de}))$	Fraction of detached leaves that is transformed into silent RCs relative to an attached leaf in percent (si: silent; at: attached; de: detached)

2.3. Statistical Analyses

The statistical analyses were performed as outlined in Keutgen et al. [28]. The derived parameters of the saturation pulse measurements and the steady-state fluorescence were calculated and tested for outliers applying the Grubbs test (<https://contchart.com/outliers.aspx>; last accessed on 5 February 2021). In the case of an outlier identified for one of the calculated parameters, the complete measurement was eliminated from further analysis, resulting in 24 accepted saturation pulse and steady-state fluorescence measurements for control and 23 for infected detached leaves. In the case of the ‘JIP’ measurements, all 40 measurements could be used for each of the control and infected detached leaves. In addition, 20 saturation pulse and steady-state fluorescence measurements of the attached control leaves were accepted. For the final comparative analyses of parameters, the measurements were tested for normal distribution applying the Kolmogorov–Smirnov and Shapiro–Wilk tests in the SPSS program SPSS® Statistics Version 26; (IBM®; New York, NY, USA).

In the case of a normal distribution, the variances were compared by F-tests and, based on the results, *t*-tests were performed, either using the conventional *t*-test or, in the case of unequal variances, the Welch–Satterthwaite method, as implemented in the Excel version of Microsoft Office 2013. In the case of a normality test not confirming the normal distribution of measurements, the Mann–Whitney U test was applied.

3. Results

In the current study, measurements were performed 6–7 days after infiltration of the leaves, but visible symptoms did not appear within 14 days, neither within nor associated to the inoculated area. The applied inoculum level of $c. 5 \times 10^5$ CFU mL⁻¹ could thus be rated as low and the response of *N. tabacum* was typical of a type-II non-host resistance.

The basic Chl-fluorescence parameters of the saturation pulse, F_0 , F_m and F_v , were significantly reduced in inoculated leaves, as were F_0' , F_m' , and F_v' (Figure 1). However, ϕ_{P0} and ϕ_{PII} were not significantly affected. ϕ_P was significantly higher in inoculated leaves. It can be broken down into q_P and ϕ_{PSII} , the latter and NPQ being similar between control and inoculated plants. PQ, q_P and the related q_L were significantly larger.

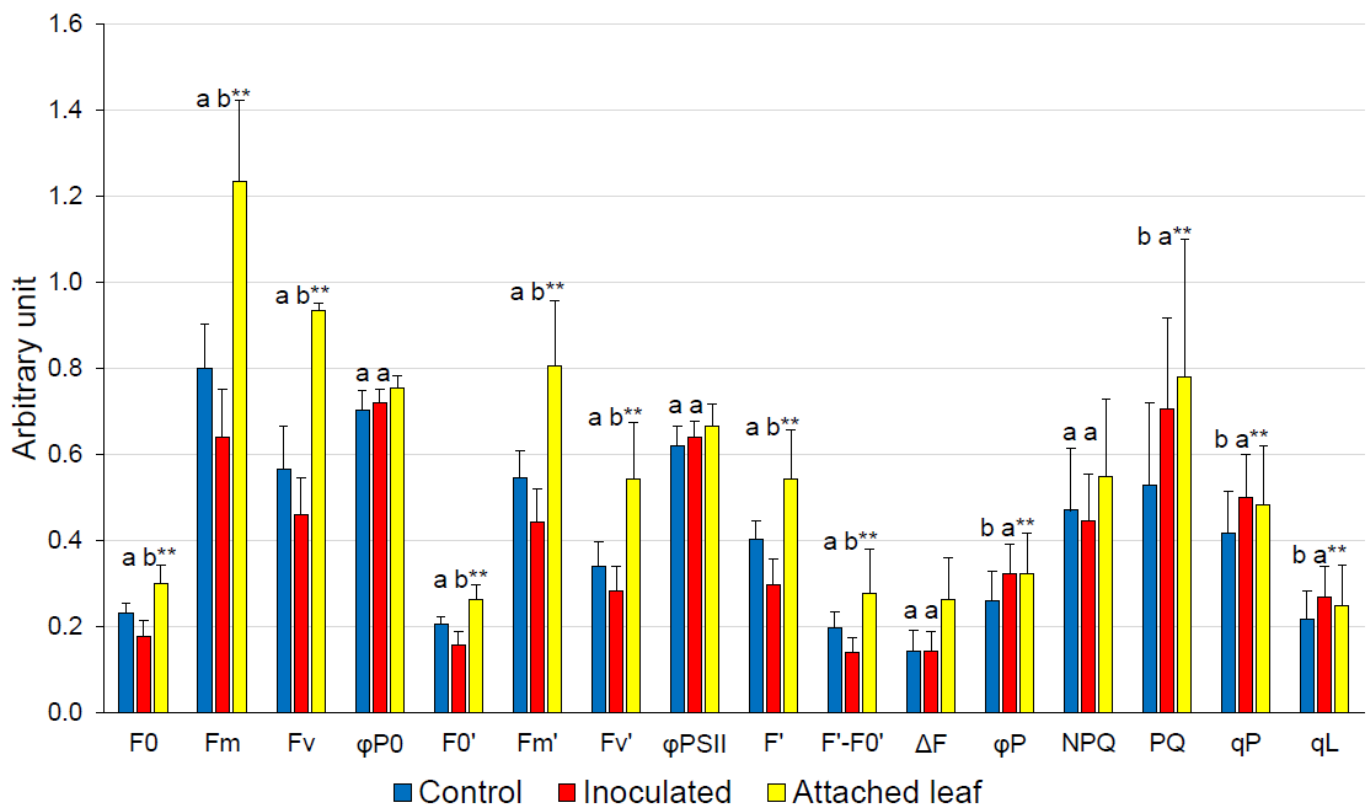


Figure 1. Saturation pulse and steady-state Chl fluorescence measurements of detached control tobacco leaves infiltrated with demineralized water ($n = 24$) and detached leaves inoculated with Pto DC3000 ($n = 23$) ($c. 5 \times 10^5$ CFU mL⁻¹) compared by *t*-tests or Mann–Whitney U tests. Measurements of untreated attached leaves are added for comparison ($n = 20$). Different letters indicate significant differences between control and inoculated detached leaves at the 5% (*) or 1% (**) significance level.

The sum of the complementary quantum yields of PSII (ϕ_P , ϕ_{NPQ1} and $\phi_{f,D1}$ of Genty et al., Cailly et al. and Hendrickson et al., and ϕ_P , ϕ_{NPQ2} , $\phi_{f,D2}$ and ϕ_{NF2} of Kornyejev and Holaday [21–24]) is defined as unity. The analyses by both approaches revealed that ϕ_{NPQ} was not significantly different between the control and inoculated leaves (Figure 2). In the case of the first approach, $\phi_{f,D1}$ was significantly smaller in inoculated leaves, compensating for the increase in ϕ_P . In the case of the second approach, $\phi_{f,D2}$ and ϕ_{NF2} were not significantly different between the control and inoculated leaves; however, the

absolute values suggest that the increase in φ_P is, to a large extent, explained by the decrease in φ_{NF2} .

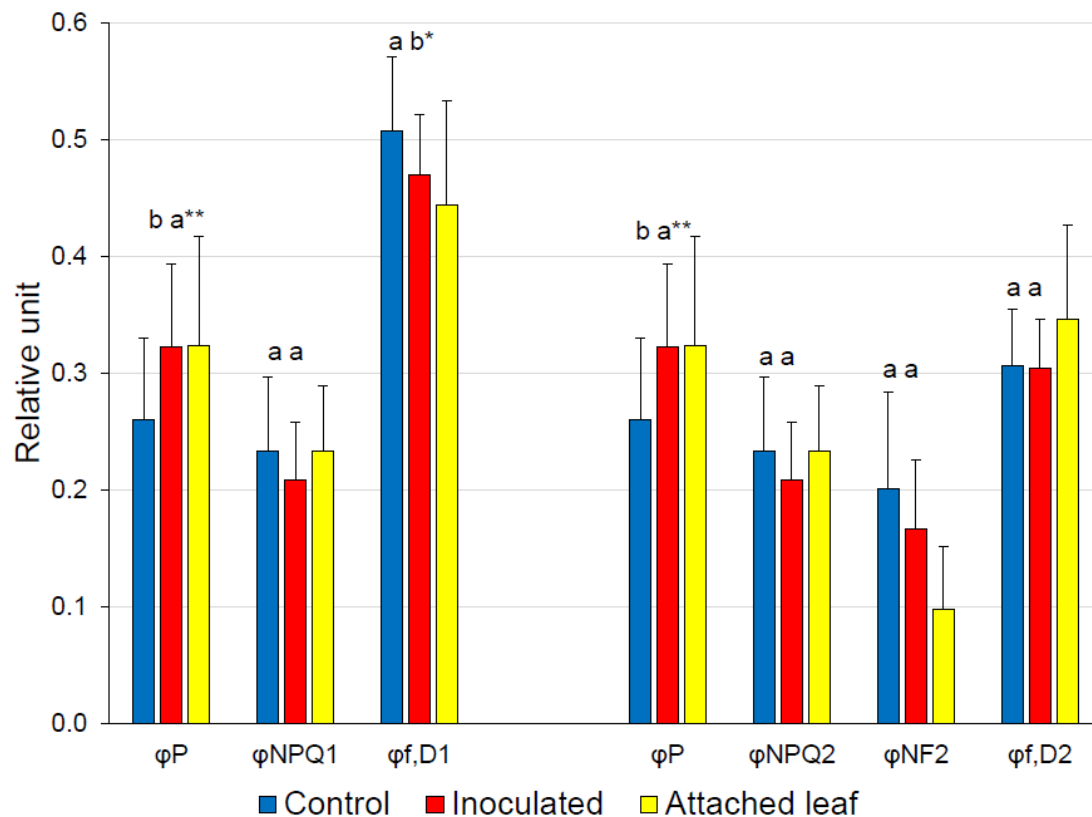


Figure 2. Energy partitioning of detached control tobacco leaves infiltrated with demineralized water ($n = 24$) and detached leaves ($n = 23$) inoculated with Pto DC3000 (c. 5×10^5 CFU mL⁻¹) compared by *t*-tests or Mann–Whitney U tests. Measurements of untreated, attached leaves are added for comparison ($n = 20$). On the left side, φ_P , φ_{NPQ1} and $\varphi_{f,D1}$ are calculated after Genty et al., Cailly et al. and Hendrickson et al. [21–23] and on the right φ_P , φ_{NPQ2} , $\varphi_{f,D2}$ and φ_{NF2} after Kornyeyev and Holaday [24] as described in Lazár [20]. Different letters indicate significant differences between control and inoculated detached leaves at the 5% (*) or 1% (**) significance level.

‘JIP’ curves of dark-adapted tobacco leaves are generally characterized by a lower fluorescence in detached leaves compared with attached leaves (Figure 3). Differences between the inoculated and control detached leaves are small, but the fluorescence of the control leaves is larger at the J-, I-, and P-steps (Figure 3). ABS/RC was not different between the inoculated and control plants, and PI_{ABS} and φ_{E0} were not significantly affected, but δ_{R0} and φ_{R0} were significantly larger in infected plants. PI_{Total} was not significantly different between the control and inoculated detached leaves, but the probability was close to the 5% level (Table 3). The transformation of RCs to so-called silent RCs as a consequence of leaf detachment was not different between the control and inoculated detached leaves.

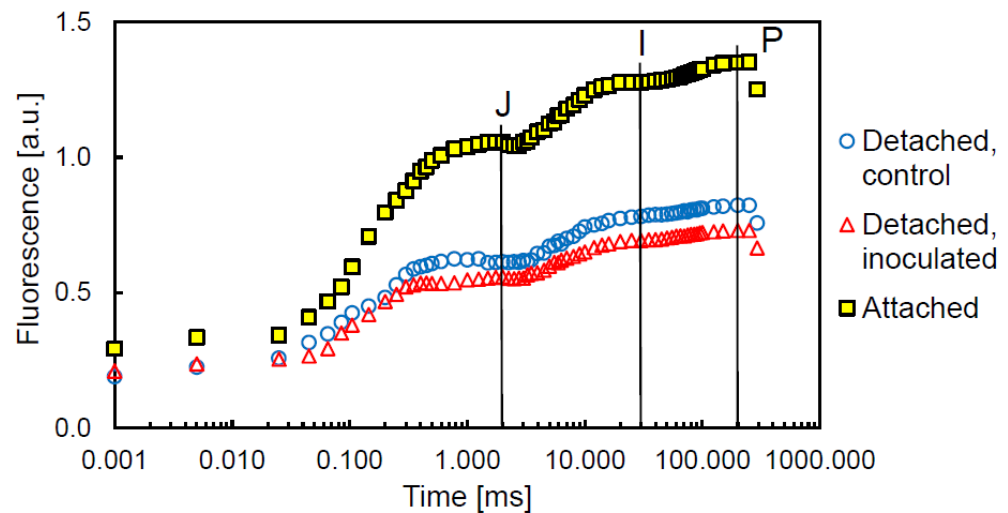


Figure 3. Fast Chl *a* fluorescence transient ('JIP' curve) of dark-adapted tobacco leaves at c. 10,000 $\mu\text{mol m}^{-1} \text{s}^{-1}$. Minimum fluorescence (F_0) was taken at the onset of fluorescence induction ($t = 0$), but is indicated in the figure for convenience at $t = 0.001$. The three curves of detached control and inoculated leaves, as well as attached leaves, represent the mean values of all measured leaves. The 'J' step was set at 2.0 ms, the 'I' step at 30 ms, and the 'P' step (or F_m) was taken at 200 ms.

Table 3. Chl-fluorescence parameters derived from measurements of the fast Chl *a* transient of tobacco leaves inoculated with Pto DC3000 compared to control leaves.

Parameter	Control	Inoculated	$P_{\text{KS-test}}$	$P_{\text{SW-test}}$	$P_{\text{F-test}}$	$P_{\text{t-test}}$	$P_{\text{MW-test}}$
ABS/RC [ms^{-1}]	4.596 ± 0.496	4.503 ± 0.604	0.002 **	0.001 **			0.117
φ_{E0} [au]	0.246 ± 0.046	0.254 ± 0.043	0.200 ^x	0.799	0.611	0.369	
δ_{R0} [au]	0.174 ± 0.037	0.196 ± 0.037	0.200 ^x	0.769	0.931	0.009 **	
φ_{R0} [au]	0.043 ± 0.013	0.050 ± 0.012	0.200 ^x	0.749	0.507	0.019 *	
PI_{ABS} [au]	0.325 ± 0.116	0.362 ± 0.139	0.200 ^x	0.949	0.260	0.211	
PI_{Total} [au]	0.072 ± 0.036	0.088 ± 0.040	0.200 ^x	0.065	0.586	0.066	
$RC_{\text{si}}/RC_{\text{at}}$ [%]	10.7 ± 9.6	8.5 ± 10.8	0.200 ^x	0.639	0.461	0.332	

Values represent means \pm standard deviation. * indicates a significance $p < 0.05$, ** a significance $p < 0.01$, ^x that this is a lower bound of the true significance, KS: Kolmogorov–Smirnov, SW: Shapiro–Wilk, MW: Mann–Whitney U [au—arbitrary unit].

4. Discussion

For the plant-pathogen system *N. tabacum*—Pto, Cheng et al. [3] reported, in the case of a high infection level, a significant decrease in φ_{P0} . By contrast, in the case of a low inoculation level, φ_{P0} was not significantly affected, which argues against a photo-inhibitory effect. When the infection level was high, the density of quinone A (Q_A)-reducing PSII RCs per cross section also decreased, indicating that the RCs, and the donor and acceptor sides of PSII, were damaged after Pto infection [3]. In the current study, φ_P and φ_{R0} were significantly higher in inoculated leaves, indicating a relatively more effective operating photosynthetic system under light conditions. The increase in φ_P was due to q_P , which may be interpreted as the fraction of open PSII RCs, but q_L is regarded as the more accurate estimate. In fact, both, q_P and q_L , and also PQ, rose (Figure 1), which is in contrast to the decrease in Q_A -reducing PSII RCs reported by Cheng et al. [3] in the case of a high infection level.

The increase in q_L , q_P , PQ and φ_P was due to a significant decrease in F' in inoculated leaves (Figure 1). The relative decrease was larger in inoculated leaves than the corresponding decrease in F_0' , resulting in a significantly smaller value for the difference $F' - F_0'$ in inoculated leaves. This implies an increased fraction of open PSII RCs in inoculated leaves, as indicated by q_L . Because ΔF was not different between the control and inoculated

leaves, in contrast to F_v and F_v' , φ_P and q_P rose significantly (Figure 1), indicating a higher efficiency in the light reactions of photosynthesis under actinic light in inoculated leaves. For comparison, the transformation of active RCs from attached to so-called silent RCs in detached leaves was calculated [29]. RC_{si}/RC_{at} is 10.7% in control leaves and 8.5% in inoculated leaves, the percentage of silent RCs between control and inoculated leaves being not significantly different (Table 3). Nevertheless, this calculation indicates that a higher number of active RCs should be expected in inoculated leaves, which would be in line with the increase in q_L .

If a saturation pulse is given to a dark-adapted leaf, all PSII RCs become closed, photochemistry is zero, and, as a consequence, excitation energy is dissipated, either as heat or fluorescence, when neglecting connectivity, spillover and oxidative damage [26]. By contrast, in the light-adapted state and in the presence of actinic light, energy partitioning is more complicated, because several processes must be considered. The advantage of an evaluation of the quantum yields of the photosynthetic energy partitioning is that the results can be compared directly, because the yields total unity. Special focus is placed on discriminating between different types of non-photochemical energy losses. Genty et al., Cailly et al. and Hendrickson et al. [21–23] identified two processes: constitutive non-regulatory basal dissipation processes consisting of fluorescence emission and heat dissipation on the one hand ($\varphi_{f,D1}$), and regulatory light-induced non-photochemical quenching (φ_{NPQ1}) on the other. Kornyejev and Holaday [24] further split $\varphi_{f,D1}$ into the quantum yield of heat dissipation by the photo-inactivated non-functional centers (φ_{NF2}) and the quantum yield of constitutive non-regulatory basal dissipation processes consisting of fluorescence emission ($\varphi_{f,D2}$, Table 1). φ_P remained similar when the inoculated detached leaves were compared to the attached leaves, whereas the φ_P of the control detached leaves was significantly smaller (Figure 2). As indicated by φ_{NPQ1} and $\varphi_{f,D1}$, the reduction in φ_P in the control detached leaves was compensated by an increase in $\varphi_{f,D1}$. Applying Kornyejev and Holaday's [24] concept, this suggests that significant differences between the control and inoculated leaves, with the exception of φ_P , were not detectable (Figure 2). Interpreting the observed tendencies with respect to the effects of leaf detachment on the one hand, and inoculation with Pto DC3000 on the other, leads to the following conclusions: leaf detachment reduced φ_P (−0.063 units) and $\varphi_{f,D2}$ (−0.040 units), but raised φ_{NF2} (+0.103 units), while inoculation resulted in an increase in φ_P (+0.062 units), compensated by a reduction in φ_{NF2} (−0.037 units) and in φ_{NPQ2} (−0.025 units) when compared with the detached control leaves.

The interpretation of the current results with respect to inoculation with Pto must consider the effect of leaf detachment. According to Weng et al. [32], detachment should result in a significantly lower φ_{P0} in detached leaves than in attached leaves, which is confirmed (Figure 1, $p < 1\%$ by t -test). Leaf detachment also reduced φ_{PSII} , φ_P (Figure 1, both $p < 1\%$ by t -tests) and $\varphi_{f,D2}$ (Figure 2, $p < 5\%$ by t -test), but increased φ_{NF2} (Figure 2, $p < 1\%$ by t -test). In summary, photosynthetic efficiency was reduced by detaching leaves and excessive energy absorbed by PSII was released as heat.

Inoculation of the detached leaves with a low infection level of Pto DC3000 resulted, when compared to the detached control, in a comparable value for φ_{P0} . Because it was hypothesized that the inoculation should affect abscisic acid (ABA) synthesis, this result was unexpected, based on Weng et al.'s [32] suggestion that leaf detachment could result in lower leaf ABA levels. In this case, inoculation of the detached leaf with Pto DC3000 should have resulted in an elevation of φ_{P0} . However, taking the evidence of McAdam and Brodribb [33] that leaf detachment itself resulted in an increase in ABA levels, the observed results may not be surprising, because an additional increase in ABA contents due to the inoculation may not have any detectable effect on φ_{P0} .

De Torres-Zabala et al. [34] supplied supporting evidence that in the host plant—pathogen system *Arabidopsis thaliana*—Pto DC3000, manipulation of the ABA hormonal network represents a fundamental step of the virulence, leading to an increase in ABA levels in the leaf. An obvious physiological benefit for the pathogen would be the ABA-

mediated stomatal closure resulting in a reduced water loss. In addition, ABA results in osmolyte accumulation and photoprotection by enhancing the xanthophyll cycle and inducing an antioxidative defense [32,34–36]. Based on the latter results, the hypothesis was proposed that, although *N. tabacum* is a non-host of Pto DC3000, the bacterium enhanced ABA content in detached tobacco leaves and, in doing so, improved the PSII efficiency of the inoculated leaves compared with that of the detached control leaves. As a matter of fact, φ_{P0} of inoculated detached leaves was by 2.3% greater than that in the control detached leaves, but this insignificant increase is not sufficient to support the hypothesis. In this context it is worthy of note that the φ_P of inoculated leaves was significantly greater (by 24%) than in control detached leaves and did not differ significantly from the φ_P of attached leaves. In addition, the φ_{PSII} of inoculated detached leaves did not differ from that of attached leaves, whereas the φ_{PSII} of the control detached leaves differed significantly from that of the attached leaves (Figure 1, $p < 1\%$ by t -test). However, the φ_{PSII} of inoculated detached leaves was only 3.3% insignificantly greater than the φ_{PSII} of the control detached leaves. Moreover, the inoculation of the detached leaves resulted in a higher fraction of active PSII RCs compared with the detached control (Figure 1, $p \cong 1\%$). In summary, these data indicate a slight, but positive, effect of inoculation with a limited amount of Pto on the efficiency of the light reactions of photosynthesis, in contrast to an infection with a high level.

Noteworthy, the φ_P of the detached inoculated leaves was similar to that of the attached leaves, but significantly greater than that of the detached control leaves (Figure 2). The increase in φ_P relative to the detached control was compensated for by a decrease in $\varphi_{f,D1}$, which may be broken down into φ_{NF2} and $\varphi_{f,D2}$. Although the differences between detached inoculated and control leaves of both parameters are insignificant, the measurements clearly exclude any treatment effect for the latter parameter (Figure 2). Consequently, the difference in φ_P between the detached inoculated and control leaves was reflected by the heat dissipation by the photo-inactivated non-functional centers (φ_{NF2}) and regulatory non-photochemical quenching (φ_{NPQ2}). It is noteworthy that the φ_{NPQ2} of the attached leaves was not significantly different from either kind of detached leaves, but the φ_{NF2} was significantly greater in detached leaves than in attached leaves (Figure 2, both $p < 1\%$ by t -tests), indicating that increased heat dissipation by the photo-inactivated non-functional centers is at least partly a consequence of leaf detachment, as is the decrease in fluorescence emission ($\varphi_{f,D2}$) (Figure 2, both $p < 5\%$ by t -tests).

In summary, the highlighted differences between control and inoculated detached leaves are the increase in photochemical efficiency (φ_P) approaching the level of an attached leaf and a higher fraction of active PSII RCs (q_L) in inoculated leaves. Seemingly, the increase in φ_P is compensated by a smaller fraction of the absorbed energy that is dissipated as heat by photo-inactivated non-functional centers (φ_{NF2}).

Another aspect is indicated by the reduction in the F_m of the dark-adapted detached inoculated leaves compared with that of the detached controls (Figure 1). F_m is frequently interpreted as a measure of the absorption of energy per excited cross section of a photosynthesizing sample at maximum fluorescence. In this respect, energy absorption of inoculated detached leaves is smaller than that of controls (and also of control attached leaves). This implies that inoculation with Pto DC3000 resulted in a reduced light absorption by the light-harvesting pigments. A lower capacity to absorb energy, but a higher fraction of active PSII RCs may be interpreted as an acclimation to limit over-excitation and to reduce heat dissipation (φ_{NF2}). The higher efficiency of inoculated leaves in the light-adapted state (φ_P) may also be related to the increased δ_{R0} , which reflects the efficiency of electron transfer from plastoquinol to the final PSI acceptors. Desotgiu et al. [37] suggested that a lower capacity to trap electrons, but a greater capacity to reduce the final electron acceptors, represents an acclimation to limit over-excitation, inducing non-photochemical de-excitation. This interpretation is reminiscent of Zivcak et al. [38], who proposed that the fraction of the light absorbed by PSII is reduced in the case of drought stress and suggested an adjustment of light harvesting between PSI and PSII. The hypothesis may be proposed that the content

of PSI relative to PSII was also larger in inoculated detached leaves, which would point to an increased cyclic electron flow in order to provide additional ATP [39], either to the bacteria or to the host plant. Because the ATP content is reduced during an HR [40], increasing ATP generation by the light reactions of photosynthesis might contribute to inhibiting an HR in the case of a low level of inoculum, or may contribute to a well-balanced ATP level in order to maintain the HR-inducing capacity [41]. These interpretations may be further examined in future studies. Disease prevention without an immediate induction of an HR, which involves a very expensive cell-death program, may be advantageous for the host plant (and also for Pto DC3000), though plants cannot tolerate a high level of inoculum. For agricultural practice, this would suggest plant protection strategies that aim at limiting pathogen proliferation, while simultaneously maintaining light reactions of photosynthesis.

The present study intended to identify responses of the light reactions of photosynthesis due to a low inoculation level of *N. tabacum* leaves with Pto DC3000. It was hypothesized that such an approach should reveal slight differences when compared with a high inoculation level resulting in an HR, elucidating additional plant strategies to cope with a pathogen infection. The incompatible interaction was selected, because such an interaction would represent a potential goal for any kind of crop plant—pathogen interactions, considering the concept of sustainable agriculture. A response stabilizing the light reactions of photosynthesis was detected after inoculation with a low inoculation level (c. 5×10^5 CFU mL⁻¹) and visible symptoms did not appear within 14 days after inoculation. Future studies should investigate the extent to which low inoculation levels of Pto DC3000 on attached leaves are tolerated by potential host plants, ideally under natural environmental conditions. Such studies should also investigate whether low inoculation levels of Pto DC3000 on attached leaves are able, possibly together with indigenous plant pathogen suppressive microbial communities, to induce a sufficient resistance against other more virulent infections. This may constitute a biological approach to controlling pests or pathogens, and potentially might become a significant component of sustainable agriculture, since prior exposure to eliciting organisms frequently rendered plants more tolerant to subsequent infections [15].

5. Conclusions

In times of climate change, the environmental conditions for the partners in a host plant—pathogen system change in an unpredictable way; as a consequence, sustainable agriculture is a difficult, but even more necessary, undertaking in reducing or optimizing the use of pesticides. It is, therefore, of fundamental importance to understand the natural mechanisms and use them for the cultivation of crop plants. This study focused on infection with a low level of inoculate; it contributes to a better understanding of the balance between a host plant and a pathogen, because these conditions resemble those observed in the field [42]. The current study may be recommended for use as a model in future studies into other economically important crops plants. For the experiment described here, it became evident that a low level of inoculation (c. 5×10^5 CFU mL⁻¹) of *N. tabacum* with Pto DC3000 led to a modification in the light reactions of photosynthesis: the lower energy absorption capacity combined with a higher proportion of open PSII RCs is interpreted as acclimatization to limit over-excitation and reduce heat dissipation. This should limit the production of reactive oxygen species and reduce the likelihood of an HR. In the experiment presented here, no visible symptoms (chlorosis or necrosis) were observed within 14 days after inoculation. Compared with the results of Rodríguez-Moreno et al. [6], this indicates that, if at all, there was only a very small increase and spread of *P. syringae* beyond the inoculated area.

Author Contributions: Conceptualization, N.K., M.T.-S. and A.J.K.; methodology, N.K. and M.T.-S.; validation, M.T.-S. and A.J.K.; formal analysis, M.T.-S., T.L. and A.F.; investigation, N.K. and M.T.-S.; resources, M.T.-S. and A.J.K.; data curation, N.K. and M.T.-S.; writing—original draft preparation, M.T.-S. and N.K.; writing—review and editing, A.J.K. and T.L.; visualization, N.K.; supervision, A.J.K. and M.T.-S.; project administration, M.T.-S., T.L. and A.J.K.; funding acquisition, M.T.-S. and A.F. All authors have read and agreed to the published version of the manuscript.

Funding: This research received no external funding.

Institutional Review Board Statement: Not applicable.

Data Availability Statement: The data are stored on the BOKU University server and will be made available on request for non-commercial studies.

Conflicts of Interest: The authors declare no conflict of interest.

References

- Wei, C.F.; Kvitko, B.H.; Shimizu, R.; Crabill, E.; Alfano, J.R.; Lin, N.C.; Martin, G.B.; Huang, H.C.; Collmer, A. A *Pseudomonas syringae* pv. *tomato* DC3000 mutant lacking the type III effector HopQ1-1 is able to cause disease in the model plant *Nicotiana benthamiana*. *Plant J.* **2007**, *51*, 32–46. [CrossRef] [PubMed]
- Mysore, K.S.; Ryu, C.M. Nonhost resistance: How much do we know? *Trends Plant Sci.* **2004**, *9*, 97–104. [CrossRef]
- Cheng, D.D.; Zhang, Z.S.; Sun, X.B.; Zhao, M.; Sun, G.Y.; Chow, W.S. Photoinhibition and photoinhibition-like damage to the photosynthetic apparatus in tobacco leaves induced by *Pseudomonas syringae* pv. *Tabaci* under light and dark conditions. *BMC Plant Biol.* **2016**, *16*, 29. [CrossRef]
- Pérez-Bueno, M.L.; Pineda, M.; Díaz-Casado, E.; Barón, M. Spatial and temporal dynamics of primary and secondary metabolism in *Phaseolus vulgaris* challenged by *Pseudomonas syringae*. *Physiol. Plant.* **2015**, *153*, 161–174. [CrossRef] [PubMed]
- Bonfig, K.B.; Schreiber, U.; Gabler, A.; Roitsch, T.; Berger, S. Infection with virulent and avirulent *P. syringae* strains differentially affects photosynthesis and sink metabolism in *Arabidopsis* leaves. *Planta* **2006**, *225*, 1–12. [CrossRef]
- Rodríguez-Moreno, L.; Pineda, M.; Soukupová, J.; Macho, A.P.; Beuzón, C.R.; Barón, M.; Ramos, C. Early detection of bean infection by *Pseudomonas syringae* in asymptomatic leaf areas using chlorophyll fluorescence imaging. *Photosynth. Res.* **2008**, *96*, 27–35. [CrossRef] [PubMed]
- Ranty, B.; Aldon, D.; Cotellet, V.; Galaud, J.P.; Thuleau, P.; Mazars, C. Calcium sensors as key hubs in plant responses to biotic and abiotic stresses. *Front. Plant Sci.* **2016**, *7*, 327. [CrossRef]
- Baxter, A.; Mittler, R.; Suzuki, N. ROS as key players in plant stress signalling. *J. Exp. Bot.* **2014**, *65*, 1229–1240. [CrossRef]
- Nguyen, D.; Rieu, I.; Mariani, C.; van Dam, N.M. How plants handle multiple stresses: Hormonal interactions underlying responses to abiotic stress and insect herbivory. *Plant Mol. Biol.* **2016**, *91*, 727–740. [CrossRef]
- Thevenet, D.; Pastor, V.; Baccelli, I.; Balmer, A.; Vallat, A.; Neier, R.; Glauser, G.; Mauch-Mani, B. The priming molecule β -aminobutyric acid is naturally present in plants and is induced by stress. *New Phytol.* **2017**, *213*, 552–559. [CrossRef]
- Pathak, R.; Singh, S.K.; Tak, A.; Gehlot, P. Impact of climate change on host, pathogen and plant disease adaptation regime: A review. *Biosci. Biotechnol. Res. Asia* **2018**, *15*, 529–540. [CrossRef]
- Atkinson, N.J.; Urwin, P.E. The interaction of plant biotic and abiotic stresses: From genes to the field. *J. Exp. Bot.* **2012**, *63*, 3523–3543. [CrossRef] [PubMed]
- Boonekamp, P.M. Are plant diseases too much ignored in the climate change debate? *Eur. J. Plant Pathol.* **2012**, *133*, 291–294. [CrossRef]
- Kumar, A.; Kumar, S.; Kumar, R.; Kumar, R.; Imran, M. Impact of climate change on plant diseases and their management strategies. *J. Pharmacogn. Phytochem.* **2017**, *6*, 779–781. Available online: <https://www.phytojournal.com/archives/2017/vol6issue6S/PartR/SP-6-6-176.pdf> (accessed on 14 September 2022).
- Hanemian, M.; Zhou, B.; Deslandes, L.; Marco, Y.; Tremousaygue, D. *Hrp* mutant bacteria as biocontrol agents: Toward a sustainable approach in the fight against plant pathogenic bacteria. *Plant Signal. Behav.* **2013**, *8*, e25678. [CrossRef]
- Velásquez, A.C.; Castroverde, C.D.M.; He, S.Y. Plant–pathogen warfare under changing climate conditions. *Curr. Biol.* **2018**, *28*, R619–R634. [CrossRef]
- CORESTA—Cooperation Centre for Scientific Research Relative to Tobacco. *A Scale of Coding Growth in Tobacco Crops*; CORESTA Guide No. 7; CORESTA: Paris, France, 2019; p. 15. Available online: <https://www.coresta.org/scale-coding-growth-stages-tobacco-crops-29211.html> (accessed on 14 September 2022).
- Oxborough, K.; Baker, N.R. Resolving chlorophyll a fluorescence images of photosynthetic efficiency into photochemical and non-photochemical components—Calculation of qP and Fv'/Fm' without measuring Fo' . *Photosynth. Res.* **1997**, *54*, 135–142. [CrossRef]
- Murchie, E.H.; Lawson, T. Chlorophyll fluorescence analysis: A guide to good practice and understanding some new applications. *J. Exp. Bot.* **2013**, *64*, 3983–3998. [CrossRef]
- Lazár, D. Parameters of photosynthetic energy partitioning. *J. Plant Physiol.* **2015**, *175*, 131–147. [CrossRef]

21. Genty, B.; Harbinson, J.; Cailly, A.L.; Rizza, F. Fate of excitation at PSII in leaves: The non-photochemical side. In *Book of Abstract, Proceedings of the Third BBSRC Robert Hill Symposium on Photosynthesis, 31 March–3 April 1996, Abstract P 18*; Department of Molecular Biology and Biotechnology, University of Sheffield: Sheffield, UK.
22. Cailly, A.L.; Rizzal, F.; Genty, B.; Harbinson, J. Fate of excitation at PSII in leaves, the nonphotochemical side. *Plant Physiol. Biochem.* **1996**, *86*.
23. Hendrickson, L.; Furbank, R.T.; Chow, W.S. A simple alternative approach to assessing the fate of absorbed light energy using chlorophyll fluorescence. *Photosynth. Res.* **2004**, *82*, 73–81. [[CrossRef](#)] [[PubMed](#)]
24. Kornyejev, D.; Holaday, A.S. Corrections to current approaches used to calculate energy partitioning in photosystem 2. *Photosynthetica* **2008**, *46*, 170–178. [[CrossRef](#)]
25. Kalaji, H.M.; Schansker, G.; Ladle, R.J.; Goltsev, V.; Bosa, K.; Allakhverdiev, S.I.; Brestic, M.; Bussotti, F.; Calatayud, A.; Dąbrowski, P.; et al. Frequently asked questions about in vivo chlorophyll fluorescence: Practical issues. *Photosynth. Res.* **2014**, *122*, 121–158. [[CrossRef](#)] [[PubMed](#)]
26. Kalaji, H.M.; Schansker, G.; Brestic, M.; Bussotti, F.; Calatayud, A.; Ferroni, L.; Goltsev, V.; Guidi, L.; Jajoo, A.; Li, P.; et al. Frequently asked questions about chlorophyll fluorescence, the sequel. *Photosynth. Res.* **2017**, *132*, 13–66, Erratum in *Photosynth. Res.* **2017**, *132*, 67–68. [[CrossRef](#)]
27. Kalaji, H.M.; Goltsev, V.N.; Žuk-Gołaszewska, K.; Zivcak, M.; Brestic, M. *Chlorophyll Fluorescence: Understanding Crop Performance—Basics and Applications*; CRC Press: Boca Raton, FL, USA, 2017. [[CrossRef](#)]
28. Keutgen, N.; Tomaszewska-Sowa, M.; Keutgen, A.J. Chlorophyll fluorescence of *Nicotiana tabacum* expressing the green fluorescent protein. *Photosynthetica* **2020**, *58*, 275–282. [[CrossRef](#)]
29. Strasser, R.J.; Tsimilli-Michael, M.; Srivastava, A. Analysis of the chlorophyll a fluorescence transient: Chlorophyll a fluorescence. In *Advances in Photosynthesis and Respiration*; Papageorgiou, G.C., Govindjee, Eds.; Springer: Dordrecht, The Netherlands, 2004; Volume 19, pp. 321–362. [[CrossRef](#)]
30. Strasser, R.J.; Tsimilli-Michael, M.; Qiang, S.; Goltsev, V. Simultaneous in vivo recording of prompt and delayed fluorescence and 820-nm reflection changes during drying and after rehydration of the resurrection plant *Haberlea rhodopensis*. *BBA-Bioenergetics* **2010**, *1797*, 1313–1326. [[CrossRef](#)]
31. Stirbet, A.; Lazár, D.; Kromdijk, J.; Govindjee. Chlorophyll a fluorescence induction: Can just a one-second measurement be used to quantify abiotic stress responses? *Photosynthetica* **2018**, *56*, 86–104. [[CrossRef](#)]
32. Weng, J.H.; Chien, C.T.; Chen, C.W.; Lai, X.M. Effects of osmotic- and high-light stresses on PSII efficiency of attached and detached leaves of three tree species adapted to different water regimes. *Photosynthetica* **2011**, *49*, 555–563. [[CrossRef](#)]
33. McAdam, S.; Brodribb, T. Mesophyll cells are the main site of abscisic acid biosynthesis in water-stressed leaves. *Plant Physiol.* **2018**, *177*, 911–917. [[CrossRef](#)]
34. De Torres-Zabala, M.; Truman, W.; Bennett, M.H.; Lafforgue, G.; Mansfield, J.W.; Rodriguez Egea, P.; Bögre, L.; Grant, M. *Pseudomonas syringae* pv. *tomato* hijacks the *Arabidopsis* abscisic acid signalling pathway to cause disease. *EMBO J.* **2007**, *26*, 1434–1443. [[CrossRef](#)]
35. Jia, H.; Lu, C. Effects of abscisic acid on photoinhibition in maize plants. *Plant Sci.* **2003**, *165*, 1403–1410. [[CrossRef](#)]
36. Lu, S.; Su, W.; Li, H.; Guo, Z. Abscisic acid improves drought tolerance of triploid bermudagrass and involves H₂O₂- and NO-induced antioxidant enzyme activities. *Plant Physiol. Biochem.* **2009**, *47*, 132–138. [[CrossRef](#)] [[PubMed](#)]
37. Desotgiu, R.; Cascio, C.; Pollastrini, M.; Gerosa, G.; Marzuoli, R.; Bussotti, F. Short and long term photosynthetic adjustments in sun and shade leaves of *Fagus sylvatica* L., investigated by fluorescence transient (FT) analysis. *Plant Biosyst.-Int. J. Deal. All Asp. Plant Biol. Off. J. Soc. Bot. Ital.* **2012**, *146* (Suppl. S1), 206–216. [[CrossRef](#)]
38. Zivcak, M.; Brestic, M.; Balatova, Z.; Drevenakova, P.; Olsovska, K.; Kalaji, H.M.; Yang, X.; Allakhverdiev, S.I. Photosynthetic electron transport and specific photoprotective responses in wheat leaves under drought stress. *Photosynth. Res.* **2013**, *117*, 529–546. [[CrossRef](#)] [[PubMed](#)]
39. Umar, M.; Uddin, Z.; Siddiqui, Z.S. Responses of photosynthetic apparatus in sunflower cultivars to combined drought and salt stress. *Photosynthetica* **2019**, *57*, 627–639. [[CrossRef](#)]
40. Mur, L.A.J.; Kenton, P.; Lloyd, A.J.; Ougham, H.; Prats, E. The hypersensitive response; the centenary is upon us but how much do we know? *J. Exp. Bot.* **2008**, *59*, 501–520. [[CrossRef](#)]
41. Vidal, G.; Ribas-Carbo, M.; Garmier, M.; Dubertret, G.; Rasmusson, A.G.; Mathieu, C.; Foyer, C.H.; De Paepe, R. Lack of respiratory chain complex I impairs alternative oxidase engagement and modulates redox signaling during elicitor-induced cell death in tobacco. *Plant Cell* **2007**, *19*, 640–655. [[CrossRef](#)]
42. Hirano, S.S.; Upper, C.D. Bacteria in the leaf ecosystem with emphasis on *Pseudomonas syringae*—a pathogen, ice nucleus and epiphyte. *Microbiol. Mol. Biol. Rev.* **2000**, *64*, 624–653. [[CrossRef](#)]